Automated condition assessment of buried sewer pipes based on digital imaging techniques

SHIVPRAKASH IYER* AND SUNIL K. SINHA
[1]Pipeline Infrastructure Research Center (PIRC) Dept. of Civil & Environmental Engineering, The Pennsylvania State University, University Park, PA 16802, USA.
email: {*shiv,sks15}@psu.edu; Phone: +1 814 883 5088; Fax: +1 814 863 7304.

Abstract

Assessing the condition of underground pipelines such as water lines, sewer pipes, and telecommunication conduits in an automated and reliable manner is vital to the safety and maintenance of buried public infrastructure. In order to fully automate the condition assessment of buried pipes, it is necessary to develop a robust defect analysis and interpretation system. This paper presents the development of an automated defect detection system for sanitary sewer pipelines using digital imaging techniques like contrast enhancement, mathematical morphology and curvature evaluation.

Keywords: Sewer pipelines, cracking, automated detection, mathematical morphology, curvature evaluation.

1. Introduction

Public infrastructure is the lifeblood of every community. The US has an estimated $20 trillion investment in civil infrastructure systems, but many of these systems are eroding due to aging, excessive demand, misuse, exposure, mismanagement and neglect. Communal sewer networks are often one of the biggest infrastructures of an industrialized country, accounting for around 3200 miles of sewers per million citizens [1]. According to the US Environmental Protection Agency and claims by other sources, there are approximately 1 million miles of sewers in the United States [2]. It has been estimated that upwards of 40% of the United States' underground infrastructure will have failed or will be on the brink of failure within 20 years, unless efforts are initiated to renew it [3, 4]. But system renewal requires adequate funding. According to an April 2000 report by the Water Infrastructure Network (WIN) Agency, "America's water and wastewater systems (underground infrastructures) face an estimated funding gap of $23 billion a year between current investments in infrastructure and the investments that will be needed annually over the next 20 years to replace aging and failing pipes and meet mandates of the Clean Water Act and Safe Drinking Water Act" [3]. This necessitates the need to monitor, detect and prevent any unforeseen failures in the working of these underground pipelines that are complex in nature.

Research in the area of highways has matured and has become the basis for studies in sewer systems. The understanding of sewer deterioration mechanisms helps asset managers

*Author for correspondence.

in developing deterioration models to estimate whether sewers have deteriorated sufficiently for likely collapses [5]. Various imaging technologies have emerged over the years and have been applied to automate inspection of pipeline systems successfully [6, 7]. Research in multisensing methods for crack detection in pavement surfaces have led to innovative ways of automating and detecting structural cracks in pipe surfaces [8]. Most municipal pipeline systems in North America are inspected visually by mobile closed circuit television (CCTV) systems to access the structural integrity of underground pipes [7]. The video images are normally examined visually and classified into grades according to the extent of damage against documented criteria. Although the human eye is extremely effective at recognition and classification, it is unreasonable to assume its suitability for assessing pipe defects in thousand of miles of pipeline images due to fatigue and subjectivity. This motivates the development of an automated pipe inspection system that can access pipe conditions to ensure accuracy, efficiency and economy in the condition assessment phase. Image preprocessing and segmentation is the initial stage for any recognition process, whereby the acquired image is partitioned into meaningful regions or segments. Therefore, it is very important to understand the basic image and model its features in order to accurately extract features of interest. As the image obtained by scanning an underground pipe is very complex in terms of its features, it is important to preprocess the image before attempting to apply segmentation and feature extraction algorithms.

This paper proposes an automated image analysis and detection methodology as an intermediate step towards complete automation of data acquisition, analysis, and eventually condition assessment based on feature classification. We propose a new approach to preprocessing image data using an improved contrast-enhancement method and final crack detection using *mathematical morphology* and curvature evaluation-based algorithm derived from digital imaging principles.

2. Automated pipe inspection

Internal inspection of pipelines is done by detection systems ranging from simple visual inspection to complex imaging systems. Some promising nondestructive diagnostic methods using infrared thermography, ground penetrating radar and pulse-echo have been used for condition assessment of sewer pipelines around the world. However, there is a common consensus that these inspection methods do not characterize the complete picture of the condition of sewers due to their dependability on unimodal data collection [2]. Although there are various destructive and nondestructive inspection methods, we will limit our discussion to the two most advanced and applicable techniques, viz. the closed-circuit television (CCTV) inspection system and the sewer scanner and evaluation technology (SSET). These methods consist of a wheeled remotely operated video camera and a lighting system. The camera platform is connected via a physical multicore cable to a remote station situated over ground. The cable is used for transmitting power supply and data, determining the distance traveled, and also allowing to manually pull the platform to safety in case of malfunction (Fig. 1). CCTV system is a cost-effective method to assure proper installation, object location, infiltration or defect in the pipeline. Detailed descriptions on different commercial platforms and CCTV cameras can be found in Morici [9]. Factors like experience of the operator, skill level, concentration and reliability of the picture quality influence the accuracy

of defect or failure diagnosis significantly. Hence, this method is suitable only for detecting gross defects that can easily be picked up in a forward vision (FV) view of the CCTV camera [2].

SSET is an innovative Japanese technology designed to nondestructively survey and inspect the interior condition of sewer pipelines. SSET uses optical scanning and gyroscopic technologies to produce a detailed digital image and provides an alternative to commonly practiced CCTV inspection methods. Figure 2 shows an SSET system with inspection probe and a typical unwrapped image. Various defects in sewer pipes are generally shown accurately, with the image resolution being adequate to clearly indicate defect type and size in most cases. At its current stage of development, SSET provides the basis for future sewer management tools that will become much more powerful as automated defect recognition software is developed [10]. SSET and CCTV provide images that are primarily in color although the SSET images are of the pipe surface scanned circumferentially as against the CCTV images that provide a forward vision of the pipe from inside. Another advantage of SSET is that it travels continuously from one man-hole section to another as it collects gyroscope data, whereas the operator needs to stop the operation when the CCTV system encounters a pipe defect in order to record it.

The methodology developed by the North America Association of Pipeline Inspectors (NAAPI) is used to quantify the sewer main condition based on video (or surface scan image) feeds. The NAAPI methodology consists of assigning a score to the cracks based on certain set criteria as discussed in the *NAAPI Manual of Sewer Condition Classification* [11]. The higher the NAAPI score, the greater is the seriousness of the cracks and higher the probability of a failure. Although pipe scan data is acquired using automated technologies like the CCTV and SSET, crack detection and classification are still done by manual operators in the field or offline which brings in the issue of subjectivity, fatigue and life-cycle cost over extended periods. Therefore, reliable automated detection and classification systems that incorporate the NAAPI scoring system without the need for a human operator

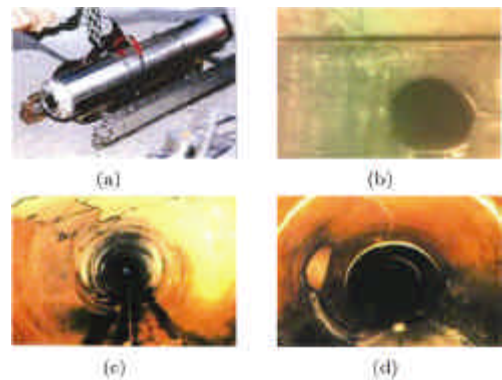FIG. 1. Schematic of buried pipe inspection system.

FIG. 2. (a) SSET inspection probe, (b) typical unwrapped digital image of a scanned pipe, and (c) and (d) forward vision (FV) images from CCTV camera.

are highly desirable under such conditions to compensate for the subjective interpretation of pipe scan images. This is a complex task because of the continuously changing pipe background scenarios, illumination and crack patterns.

3. Literature review

Most of the literature concerning the detection of defects (like cracks) in civil structures deals with the analysis of pavement and concrete/steel distress that are not directly applicable to underground pipe inspection [12]. In analyzing underground pipe scanned image data, it is imperative to consider complications due to inherent noise in the scanning process, irregularly shaped cracks, as well as the wide range of pipe background patterns. In the past two decades, many approaches have been developed to deal with the detection of linear features on retinal, satellite and most recently, underground pipe images [13–16]. Most of them combine a local criterion evaluating the radiometry on some small neighborhood surrounding a target pixel to discriminate lines from background and a global criterion introducing some large-scale a priori knowledge about the structures (e.g. cracks) to be detected.

The techniques used for pavement distress detection in scanned images are based on conventional edge or line detectors with respect to local criterion [17–19]. These methods evaluate differences of averages, thus indicating noisy results and inconsistent false-alarm rates. This necessitates the introduction of global constraints owing to insufficiency of local criterion in line and edge detection. As cracks in underground scanned pipe images resemble undulating curves with a generally constant width, Hough transform-based approaches have also been tested for the detection of parametric curves, such as straight lines or circles [20]. Tracking methods and energy minimization methods, such as snakes, have been used to track roads in satellite images and heart walls in live feeds from medical ultrasound angiographies [21, 22]. These tracking methods find a minimum cost path in a graph by using some heuristics like an entropy criterion. Statistical methods such as those that employ Bayesian framework complemented by cross-correlation detectors have been used by Fieguth and Sinha [15] to detect cracks to a reasonable accuracy level. However, their results were noisy with high false alarm rates when the image had dark background with multiple cracks in a tree-like geometry. Morphology-based filtering coupled with cross-curvature evaluation has not been used to detect cracks and remains an unexplored frontier till date. We will show that the application of some carefully selected morphological filters leads to a simplified image whose cross-curvature evaluation can be done easily for segmenting crack pixels from the image.

4. Automated crack detection

Two aspects are important from the automation of crack detection viewpoint; a contrast enhancement scheme and an effective crack segmentation methodology. In this section, we present a brief discussion on contrast enhancement, mathematical morphology and curvature evaluation before attempting to describe the implementation of our algorithm for automated crack detection.
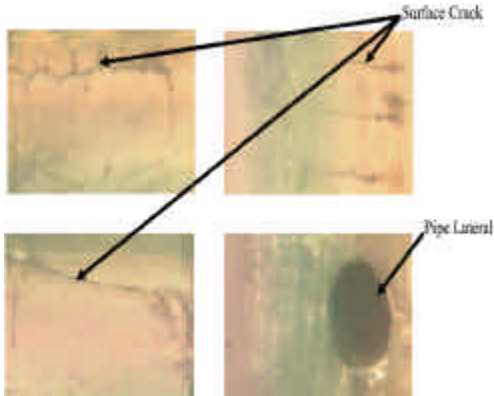
F<small>IG</small>. 3. Sample images from SSET showing different crack patterns, pipe lateral and varying illumination levels.

4.1. *Contrast enhancement*

The use of digital image data for a spatial database requires several preprocessing procedures. These procedures include, but are not limited to: geometric correction, image enhancement, and feature selection. The goal of digital image preprocessing is to increase both the accuracy and the interpretability of the digital data during the image processing phase [23]. The aim of preprocessing in underground pipeline images is an improvement of the image data that suppresses unwanted distortions in background or enhances some image features (like cracks) important for further processing. This will allow for accurate spatial assessments and measurements of crack features from the SSET or CCTV imagery.

The presence of various features in an acquired image (Fig. 3) poses considerable challenge in detecting the desired structural failure patterns such as cracks, fissures, etc. Various features make it complex for a recognition system to classify the desired patterns. Hence, this necessitates the application of low-level methods of image preprocessing to enhance the acquired image. The principal objective of image enhancement techniques is to process an image so that the result is more suitable than the original image for specific application. 'Specific' in our case applies to enhancing contrast between the background of pipe and crack features. Crack features are deeper than the pipe surface. This causes the deep regions to produce color pixels with a characteristic intensity compared to the rest of the image. We will briefly discuss our approach to contrast enhancement in Section 5.1.

4.2. *Mathematical morphology*

The techniques of mathematical morphology are based on set-theoretic concepts, on nonlinear superposition of signal, and on a class of nonlinear systems that we call morphological systems. This section is a brief review of fundamental definitions of morphological operators considered in this study. Advanced information on mathematical morphology can be found elsewhere [24–27].

For our reference, we will define a two-dimensional (2D) grayscale image having a range of $[I_{min}, I_{max}]$ as a functional $F: R^2 \to [I_{min}, I_{max}]$, and a 2D structural element as a functional

$B: R^2 \to B$ where B is the set of the neighborhoods of the origin. We consider structuring elements invariant by translation that are identified with a subset of R^2 and will be referred to as linear structuring element when this subset is a line segment. Basic morphological operators with respect to the structuring element B, a scaling factor e, image F and a processing point $P_0 \in R^2$ can be defined as:

erosion: $\boldsymbol{e}_B^e(F)(P_0) = \text{MIN}_{P \in P_0 + e \times B(P_0)}(F(P))$;
dilation: $\boldsymbol{d}_B^e(F)(P_0) = \text{MAX}_{P \in P_0 + e \times B(P_0)}(F(P))$;
opening: $\gamma_B^e(F) = \boldsymbol{d}_B^e(\boldsymbol{e}_B^e)(F)$;
closing: $\boldsymbol{f}_B^e(F) = \boldsymbol{e}_B^e(\boldsymbol{d}_B^e)(F))$;
top-hat: $TH_B^e(F) = F - \gamma_B^e(F)$

Morphological reconstruction is often presented using the notion of geodesic distance and hence the term, geodesic operators [28]. They are usually defined with reference to a geodesic distance and type of connectivity. In other words, they depend on a 'marker' image F_m (connectivity map) and a geodesic distance d.

The geodesic reconstruction (or opening) is defined by

$$\boldsymbol{g}_{F_m}^{rec}(F) = \sup(\Delta_{F_m}^d(F)), \ d \in I$$

where $(\cdot)$ is the geodesic dilation. The geodesic closing is defined by

$$\phi_{F_m}^{rec}(F) = I_{\max} - \boldsymbol{g}_{\max}^{rec} - {}_{F_m}(I_{\max} - F).$$

We assume that the tree-like geometry of cracks is the only element of our image that is locally uniform and can be described by the following properties:

- intensity distribution of a cross-section of crack looks like a specific gaussian curve;
- they branch like a tree;
- more or less have a constant width (Fig. 3).

These properties can further be classified into those related to morphological descriptions and those related to the calculation of curvature parameters based on linearity, connectivity, crack width, and gaussian profile.

4.3. *Curvature evaluation*

It is possible to study and separate the curvature characteristics of tree-like vascular structures in retinal angiographic images thus using it as a tool to segment vessels for opthalmic diagnosis (see [29] for detailed analysis and proof). Cracks in pipe scan images, like vessels in retinal angiographic images, have a tree-like structure and hence can be separated from the rest of the image using its differential properties. *Curvature* in the context of digital images is the curvature in the cross-direction defined for every pixel in the image under the assumption that any nonzero point in the picture has a dominant direction and hence can be considered as part of some crack pattern. Figure 4 schematically explains curvature properties of different elements in a pipe image. There are certain undesirable patterns encountered in the image when extracting cracks that have differential curvature characteristics. They can be classified into different cases that we will refer to in this paper:
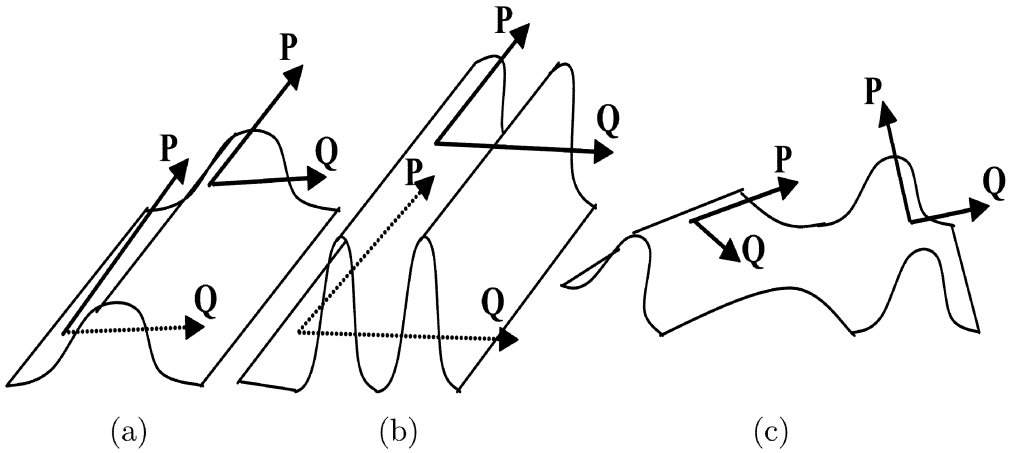
FIG. 4. (a) Crack, (b) and (c) cases 3 and 2, respectively, from Section 4.3. P and Q are the principal directions.

1. noise occurring in the data acquisition process, or due to undesirable elements whose texture can be described by a low-intensity white noise;
2. linear features in the background that can be confused with cracks in some parts, but that do not meet all the requirements;
3. dark thin irregular zones that qualify as nonlinear patterns.

In case 3 [Fig. 4(b)], the image signal appears as thin and irregular dark linear elements; therefore, the curvature takes on positive values on a width smaller than in the case of a crack (see Fig. 4(a)). It is not necessarily linearly correlated. In case 2 [Fig. 4(c)], the signal tends to be low and disorganized and the curvature will take on positive and negative values in various directions.

5. Crack detection algorithm

5.1. *Contrast enhancement of color images*

We use an approach to enhancement called *Magnification of dark image features* by increasing the contrast of the dark pixels from the estimated 'background' image. The output is the gray-scale enhanced image. The background image is the image of the pipe without any small features (e.g. cracks). Given the input color image, a median filter is applied to each of the R, G, and B component images. The median filter considers each pixel in the image in turn and looks at its nearby neighbors to decide whether or not it is representative of its surroundings (in this case, crack pixels). Instead of simply replacing the pixel value with the mean of neighboring pixel values, it replaces it with the median of those values. The median is calculated by first sorting all the pixel values from the surrounding neighborhood into numerical order and then replacing the pixel being considered with the center pixel value. We exploit this property of the median filter with an appropriate window size suitable for crack sizing and sort pixels that belong to cracks for enhancement. The window size for the median filter is 15×15. This was determined based on the width of the

crack lines. The window size is big enough to erode the small features but small enough to be computationally fast. This method picks the dark pixels by comparing the intensity of each pixel in the original color image with that of the background image. Figure 5 shows SSET images that have been contrast-enhanced by the *Magnification of dark image features* method as a preprocessing step for crack segmentation.

5.2. *Morphological treatment for the recognition of crack features*

We employ morphology-based filters with linear structuring elements taking advantage of the linear property of crack features.

A morphological closing with a linear structuring element will remove a crack or part of it when the element cannot be included in the geometry of the crack. This is true when the structuring element is orthogonally oriented with respect to the crack and is hence longer than the crack width. However, the crack will not be affected when the structural element and the crack have parallel directions. A sum of top-hats along possible directions will highlight the cracks irrespective of their inclination in the image if closings along a class of linear structuring elements are performed. But this sum of top-hats will recover a lot of noise because the closings require the structural elements to be large enough to remove unwanted features in the image that do not fall in the category of cracks. Hence, we perform reconstruction operations using connectivity property of the cracks before taking the sum of top-hats to ensure that components which do not fit the definition of cracks are removed (Fig. 6).

A geodesic reconstruction of the closed images into the original image F_0 will remove noise while preserving most of the cracks that were not removed by the closing operation. Mathematically this operation can be represented as:
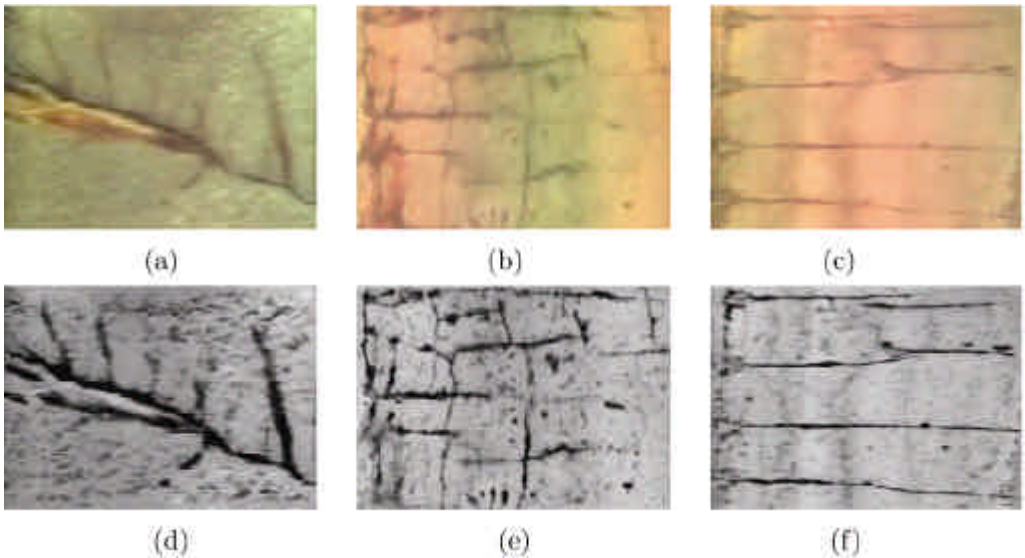

FIG. 5. Contrast enhanced images: (a), (b) and (c): original RGB color image; (d), (e) and (f): enhanced image using *Magnification of dark image features* method.

$$F_{cl} = \boldsymbol{f}_R^{12}(\text{Min}_{i=1\cdots18}\{\boldsymbol{f}_{B_i}(F_0)\}).$$

Each linear (width = 1 pixel) structuring element B_i is 12 pixel long and is oriented at every 10° from 0 to 180. The element size is based upon the range of crack widths that are of interest to the pipeline community. A more detailed discussion on this will follow in Section 6. The resulting reconstructed image F_{cl} will not have any isolated round zone whose diameter is less than the size of structuring element (12 pixels). This step, called *linear closing by reconstruction* of size 12, removes noise and other features that are not connected to the crack geometry. The sum of top-hats on the filtered image F_{cl} will enhance all cracks irrespective of their orientations including minor cracks in a low contrast image. However, the *Fcl* image contains a lot of details corresponding to cases 2 and 3 in Section 4.3.

5.3. *Final segmentation based on curvature characteristics*

It is worthwhile to recall from Section 4.3 that *curvature* is defined as the curvature in the cross-direction which is defined for every pixel under the assumption that any nonzero point in the picture has a dominant direction and hence can be considered as part of some crack pattern. Its evaluation using the Laplacian operator on a top-hats operated image has been analytically discussed and presented by Zana and Klein [29]. As discussed in Section 4.3, nonlinearly correlated patterns have signals that appear as thin and irregular dark elements indicating that the curvature gets positive values on a width smaller than in the case of the cracks (Fig. 4). In the case of details like 2 (Section 4.2), the curvature will have alternating positive and negative values in various directions owing to a low and disorganized signal. This can sometimes lead to represent a curvature trend that fits the crack description. The study does not attempt to address this issue leading to false detection in a few cases which are rare and have little bearing on the overall performance.

It has been proven that the sign of Laplacian applied to the result image of top-hats can be used as a good approximation of the sign of curvature [29]. We compute the Laplacian

FIG. 6. Steps in the morphology-based recognition process: (a) original (contrast-enhanced) image, (b) supremum of closing, (c) geodesic reconstruction, and (d) sum of top-hats.
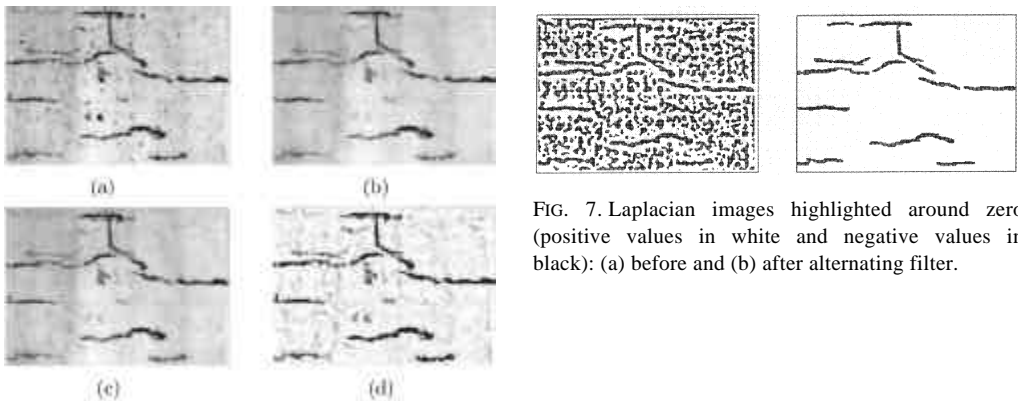

FIG. 7. Laplacian images highlighted around zero (positive values in white and negative values in black): (a) before and (b) after alternating filter.

of F_{cl} to obtain a good estimation of the curvature (see Fig. 7(a)). The final step in the detection process is the application of alternating filters that remove enhanced noise patterns corresponding to 1) and 2) as discussed in Section 4.3 thereby producing the final binary crack map. The alternating filtering operation consists of performing a linear closing by reconstruction of size 12, followed by a linear opening by reconstruction of size 12, and finally a linear closing of size 24. These sizes were chosen based on statistics generated on a database of 225 pipe images acquired from various cities in North America (rationale behind the selection of these values is discussed in Section 6). The algorithm was designed to segment cracks and remove all possible false detection under varying color, background and crack patterns based on criticality levels defined by the municipal pipeline community. A change in strategy may simply require a different alternating filter.

5.4. *Steps of the proposed algorithm*

We can summarize our algorithm as follows:

Step I: Improve the contrast of RGB pipe image by enhancing the dark pixels from the 'background' image.

Step II: Perform crack enhancement described by the following equations in mathematical morphology terms:

$$F_{cl} := f_R^{12}(\text{Min}_{i=1\cdots18}\{f_{B_i}(F_0)\});$$

$$F_{sum-th} := \sum_{i=0}^{18}(F_{cl} = f_{B_i}(F_0)).$$

The sum of top-hats reduces noise and improves the contrast of all linear regions in the image. At this stage, a manual threshold on F_{sum-th} could result in cracks being segmented out from the image, but in most cases the image would be noisy thus requiring further treatment by curvature evaluation using a Laplacian filter

$$F_{lap} := \text{Laplacian}(Gaussian_{s=2}^{width=12px}(F_{sum-th})).$$

Step III: The third step in the detection process consists of applying a set of filters with linear structuring elements to remove the enhanced noise patterns. The set of alternating filters can be described by

$$F_1 := f_R^{12}(\text{Min}_{i=1\cdots18}\{f_{B_i}(F_{lap})\});$$
$$F_2 := g_R^{12}(\text{Max}_{i=1\cdots18}\{gB_i(F_1)\});$$
$$F_{final} := (\text{Min}_{i=1\cdots18}\{f_{B_i}^2(F_2)\} \leq 1).$$

The final closing by a larger structuring element (scaling factor of 2) removes smaller and tortuous segments of cracks that are shorter than the structure element. Cracks are readily identified as pixels whose values are larger than a small positive value such as 1 (Fig. 7).

6. Discussion on the robustness and accuracy of the proposed algorithm

6.1. *Pipe image database*

The algorithm has been adapted to other types of pipe images: background variations, crack patterns, and color variations based upon the geographical location and condition of pipe.

Background variations are a result of changing illumination and maintenance conditions for a given pipeline whereas color variations depend upon the material used for the pipeline, viz. clay or concrete. Development of vegetation or algae can also add to the background color patterns. In such images, cracks are less contrasted than in images where the background is generally linear.

Careful observation reveals that the crack patterns in pipe scan images reveal a certain extent of damage in that section of pipe. Usually, the probability that there is no crack in a section of pipe is very high as compared to the presence of crack. Thus, crack recognition and segmentation is of utmost interest from an image registration point of view for future applications in 3D crack visualization and feature selection for accurate pipe condition assessment.

6.2. *Evaluation of the proposed algorithm*

It is necessary to evaluate the performance of our algorithm on images with varying crack pattern, color and background as the case may be in the field. The evaluation is carried out by comparing cracks detected automatically with manually plotted cracks (ground truth). A set of connected pixels belonging to the cracks is manually extracted using an inhouse GUI interface to replicate the process carried out by a pipe inspector in the field. We use the 'buffer-method' for performance evaluation by matching the automatically extracted crack pixels to the reference map or ground truth image [30]. This method is a simple matching procedure in which a buffer of constant predefined width is constructed around the crack data in two steps. In the first step, a buffer of constant width is constructed around the reference crack data by using a morphological dilation operation of size 5×5 (Fig. 8). The parts of the extracted data within the buffer are considered as matched and are denoted as *true positive*, whereas the unmatched extracted data is denoted as *false positive*. In the second step, the matching is performed the other way round by constructing a buffer of the same size around the extracted crack data (Fig. 8) and the part of reference data lying in the buffer is considered as matched. The unmatched reference data is denoted as *false negative*. Probability of detection is defined as the ratio of detected crack pixels to true crack pixels and probability of false alarm is the ratio of false alarm pixels to noncrack pixels in the image. Figure 8 illustrates the matching procedure to quantitatively determine the probability of detection P_d and probability of false-alarm P_{fa} (false +ve and –ve).

6.3. *Selection of algorithm parameters*

The size of structuring element and degree of rotation are two prime parameters that govern the performance of the proposed algorithm. It is imperative to discuss the detection probabilities as a function of these two parameters. Generalization to images of all types can only be effected if algorithm performs very well under varying image conditions. Hence, an optimum parameter combination is required that can consistently provide high detection probabilities under all conditions based on a set criteria for P_d and P_{fa} as suggested by the concerned authorities. In order to quantitatively assess the effect of structuring element size and degree of rotation on the detection rate, we plot the probability of detection (P_d) against the probability of false alarm (P_{fa}) for different structuring element sizes and degree of rotations. We performed experiments on three different classes of pipe images (crack patterns, background and color) by varying the size of structuring element (S = 10, 12 and 15 pixels)

and degree of rotations (D = every 5°, 10° and 15°) to determine an optimum combination of these two parameters. Given a low false +ve (7%) and false −ve (2%), the corresponding size of structural element and degree of rotation that gives the maximum P_d is selected. This is repeated for all the three classes of image and the candidate combination that satisfies the cutoff criteria throughout is finally selected as the generalized optimum parameter combination. Figure 9 shows the probabilities plotted against various parameter combinations for images with varying crack patterns, background and color. S12-D10 (structural elements of size 12 px rotated at every 10°) clearly satisfies the cutoff criteria and is selected as the optimum combination that consistently provides good detection in all types of pipe images.

6.4. *Experimental results*

This algorithm has been tested on a database of about 225 images of all types taken from various cities like Los Angeles, Albuquerque, Toronto and St Louis-Missouri in North America. All the images were acquired and unwrapped using the SSET camera and its pro-
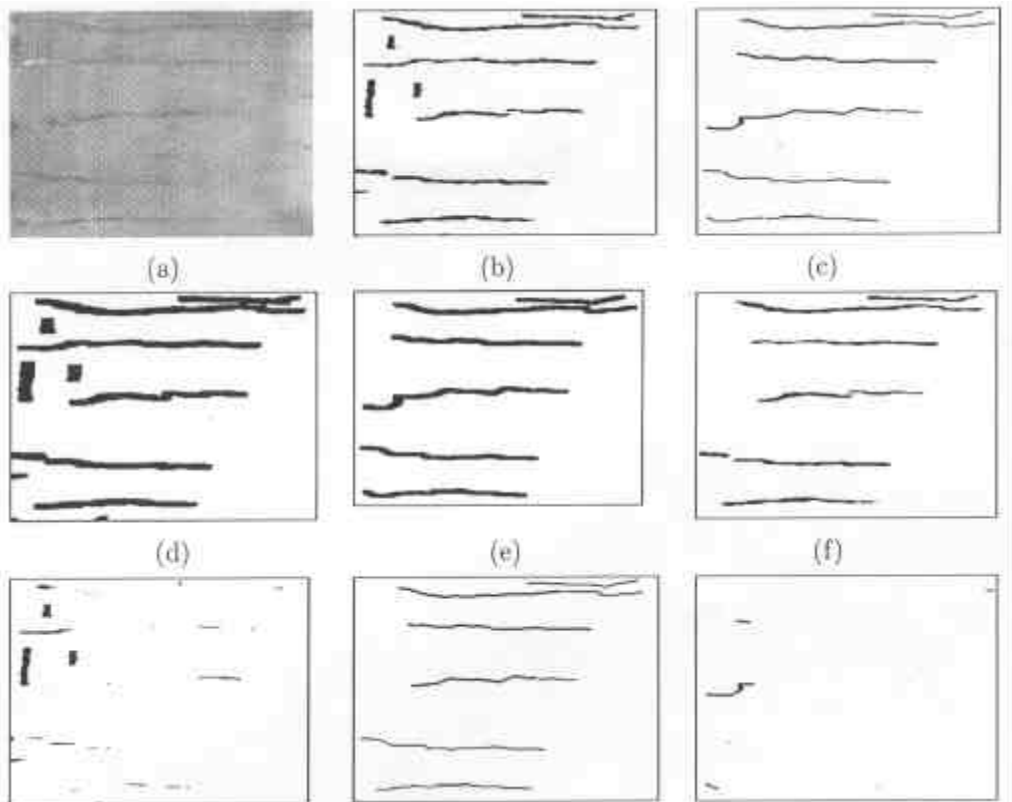
FIG. 8. Matching procedure for detection of true and false pixels. (a) original image, (b) detected cracks, (c) ground truth, (d) and (e) detected and true cracks dilated by a 5 × 5 structuring element, (f) good points of the filter, (g) false +ve, (h) truly detected cracks and (i) missed cracks (false −ve).
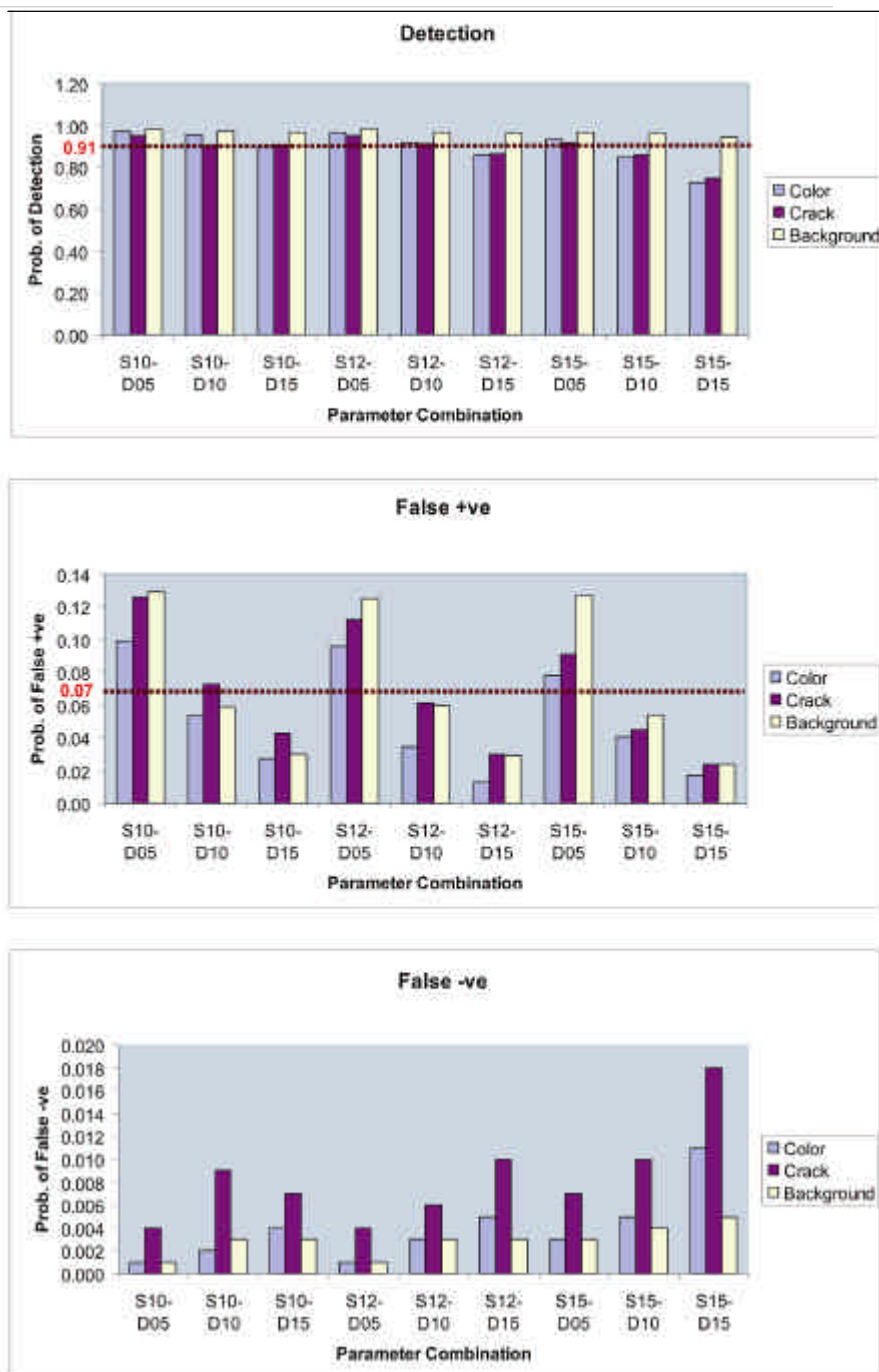
FIG. 9. Bar chart of probabilities for different parameter combinations. S12-D10 consistently meets criteria in all the three classes.
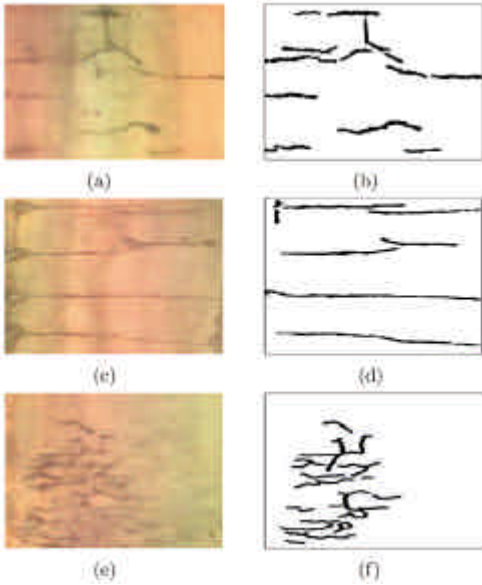
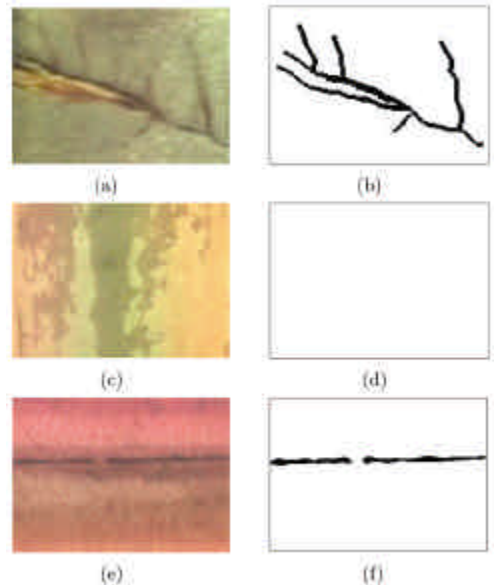FIG. 10. Image with different crack patterns.

FIG. 11. Image with different background patterns.

prietory software available with the system. Robustness was evaluated on noisy images with respect to changing crack patterns (Fig. 10), background features (Fig. 11) and color (Fig 12). Images that did not have any cracks present produced a perfect image without any detected cracks every single time the algorithm ran with the generalized optimal parameter combination.

There has been false detection in the following cases:

• extension of crack into a small rounded zone (patch) maintaining the same direction and geometry;

• cracks are too close to each other;

• dark linear structures mistaken for cracks that appear as isolated objects in the image;

• uniform noise that would modify the connectivity of crack structure thereby disturbing the reconstruction filter and misleading curvature evaluation.

Parts of the crack were not detected mostly in very low contrast (Fig. 12) and sometimes in images that had shadow due to illumination issues in the pipe. However, the detection in every case was in accordance with the discussion in Section 6. This algorithm works on detecting patterns with Gaussian profile bounded at the inflection point. The Gaussian filter applied before the computation of the Laplacian modifies the surrounding texture leading to a shift in the location of the inflection point. As a consequence, our experiments show that small cracks appear wider than their real size (Fig. 10). However, this is not a matter of major concern as detection is based on matching the extraction with respect to a buffer width as discussed in Section 6.2.
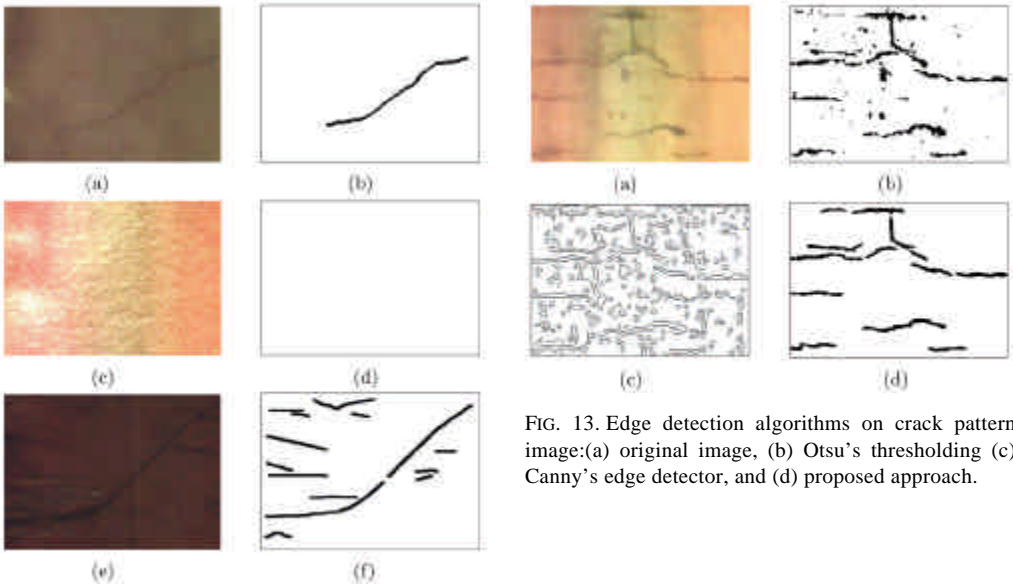
FIG. 13. Edge detection algorithms on crack pattern image:(a) original image, (b) Otsu's thresholding (c) Canny's edge detector, and (d) proposed approach.

FIG. 12. Image with different color variations.

6.5. *Comparison of the proposed algorithm with other methods*

We apply several detection filters to an original image including our proposed algorithm to study the performance with respect to other conventional filters used in the underground pipeline infrastructure industry. We have used Canny's edge detec   d-ing technique to extract crack features [31, 32]. Figures 13–15 show comparative results from the application of our proposed approach, Canny's edge detection method, and Otsu's thresholding technique to a sample image from all three classes (color, background and varying crack patterns).

The Canny edge detector produces parallel edges (Figs 13, 14 and 15(c)) suggesting that the largest cracks are easily picked up by the detector at the cost of smaller cracks that appear less contrasted. Otsu's thresholding technique selects a threshold based on integration (a global property) of the gray-level histogram. Hence, in areas where the cracks and background path run into each other or low contrast dark images, false detection is inevitable as seen in Figs 13 and 15(b). Images in Figs 13 and 14(a) that show minor and major cracks are part of sewer pipeline system in Boston and Los Angeles, respectively. The crack detection step performs quite well detecting most of the crack structures, while missing only some micro-cracks in the images. These cracks might have been present at the time of manufacturing of the pipe and are not a threat to the structural integrity according to industry experts. The image in Fig. 15(a) belongs to a sewer pipeline system in St Louis, Missouri, and has dark pipe surface (clay pipe) with a major crack camouflaged in the background in addition to minor cracks. Although there is little contrast between the background and crack features, the crack detection step performed well only missing some minor cracks. Performance evaluation of minor cracks in complex images (Fig. 15(a)) is not easy because it is difficult even for a trained human operator to identify such minor cracks.
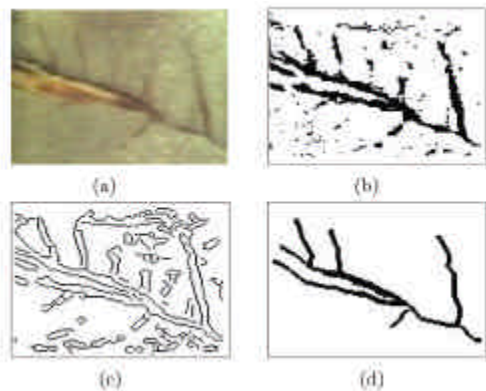
FIG. 14. Edge detection algorithms on background pattern image: (a) original image, (b) Otsu's thresholding, (c) Canny's edge detector, and (d) proposed approach.
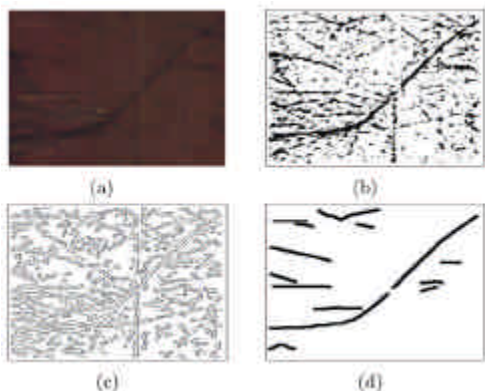
FIG. 15. Edge detection algorithms on color variation image: (a) original image, (b) Otsu's thresholding, (c) Canny's edge detector, and (d) proposed approach.

7. Conclusions

Automated crack detection systems that limit the necessity of human inspection have the potential to lower the life-cycle cost of condition assessment of buried pipes. In this paper, we have adapted and implemented an efficient algorithm for detecting crack patterns in pipeline images. This automated method can be divided into three steps, viz. contrast enhancement, morphological treatment and curvature evaluation in the cross-direction and finally the alternating filters that produce the final segmented binary crack map. The proposed evaluation scheme adequately estimates the performance of this algorithm in an absolute way and is relative to conventional detection techniques used in the underground pipeline inspection industry. The robustness and weaknesses of the algorithm have been discussed in order to facilitate its use in a larger scheme for condition assessment of underground pipelines. The scope of this article is focused on improving the segmentation methodology in pipeline images. Further development of this algorithm in terms of defect feature classification needs to be actively pursued in preparation towards an automated condition assessment tool.

References

1. O. Duran, K. Althoefer and L. D. Seneviratne, State of the art in sensor technologies for sewer inspection, *IEEE Sensors J.*, **2**, 73–81 (2002).

2. M. J. Chae, and D. M. Abraham, Neuro-fuzzy approaches for sanitary sewer pipeline condition assessment, *ASCE J. Comp. Civ. Engng.*, **15**, 4–14 (2001).

3. Water Infrastructure Network (WIN) Agency Report (2001).

4. Water Infrastructure Network (WIN) Agency Report (2002).

5. R. Wirahadikusumah, D. M. Abraham and T. Iseley, Challenging issues in modeling deterioration in combined sewers, *ASCE J. Infra. Syst.*, **7**, 77–84 (2001).

6. C. Haas, Y. Kim and R. Greer, A model for imaging assisted automation of infrastructure maintenance, *Proc. Second Int. Conf. on Imaging Technologies and Applications in Civil Engineering*, Davos, Switzerland, pp. 108–117 (1997).

7. S. R. Gokhale, D. M. Abraham, and T. Iseley, Intelligent sewer condition–Evaluation technologies. An analysis of three promising options, *North American No-Dig 1997 Conf.*, North American Society for Trenchless Technology, pp. 253–265 (1997).

8. D. Gharpuray, and C. Haas, A comparison of multi-sensing methods for the detection of cracks in pavement surfaces, *Pacific Rim Trans. Tech Conf.*, Vol. 7, pp. 425–429 (1993).

9. P. Morici, Small cameras: diagonizing sewer laterals quickly and easily, *Trenchless Technol.*, **6**(10), pp. 40–45 (1997).

10. Evaluation of SSET: The sewer scanner and evaluation technology, A technical report, http: //www:cerf:org (2001).

11. Pipeline assessment and certification program (PACP), Training Manual, National Association of Sewer Service Companies (NASSCO) (2001).

12. H. D. Cheng, and M. Miyogim, Novel system for automatic pavement distress detection, *J. Computing Civil Engng*, **12**, 145–152 (1998).

13. N. Merlet, and J. Zerubia, New prospects in line detection by dynamic programming, *IEEE Trans. PAMI,* **8**, 426–431 (1996).

14. O. Hellwich, M. Mayer, and G. Winkler, Detection of lines in synthetic aperture radar (SAR) scenes, *Proc. Int. Archives Photogrammetry Remote Sensing (ISPRS)*, Austria, Vol. 31, pp. 312–320 (1992).

15. P. W. Fieguth, and S. K. Sinha, Automated analysis and detection of cracks in underground scanned pipes, *Proc. Int. Conf. Image Processing (ICIP)*, pp. 395–399 (1999).

16. R. Sharpe, J. Gilbert, and S. Oakes, Expert systems and artificial intelligence applications in engineering design and inspection, *8th Int. Conf. on Ind. & Engng Applications of AI & Expert Systems*, International Society of Applied Intelligence (ISAI), pp. 99–109 (1995).

17. M. H. Mohajeri, and P. J. Manning, ARIA^{TM}: An operating system of pavement distress diagnosis by image processing, *Transportation Res. Record*, 1311, 120–130 (1991).

18. R. S. Walker, and R. L. Harris, Noncontact pavement crack detection system, *Transportation Res. Record*, 1311, 149–157 (1991).

19. H. N. Koutsopoulos, I. E. Sanhouri, and A. B. Downey, Analysis of segmentation algorithms for pavement distress images, *ASCE J. Transportation Engng*, **119**, 868–888 (1993).

20. J. Skingley, and A. J. Rye, The Hough transform applied to images for thin line detection, *Pattern Recognition Lett.*, **6**, 61–67 (1987).

21. D. Geman, and B. Jedynak, An active testing model for tracking roads in satellite images, *IEEE Trans. PAMI*, **18**, 1–14 (1996).

22. M. Kass, A. Witkin, and D. Terzopoulos, Snakes: Active contour models, *Int. J. Computer Vision*, **1**, 321–331 (1988).

23. R. C. Gonzalez, and R. E. Woods, *Digital image processing*, 2nd edn, Pearson Education, Singapore (2002).

24. J. Serra, *Image analysis and mathematical morphology*, Academic (1982).

25. J. Serra, *Image analysis and mathematical morphology–Theoretical Advances*, Vol. 2, Academic Press (1988).

26. G. Matheron, *Random sets and integral geometry*, Wiley (1975).

27. P. Maragos, and R. W. Schafer, Morphological systems for multidimensional signal processing, *Proc. IEEE*, **78**, 690–710 (1990).

28. L. Vincent, Morphological grayscale reconstruction in image analysis: Applications and efficient algorithms, *IEEE Trans. Image Processing*, **2**, 176–201 (1993).

29. F. Zana, and J. C. Klein, Segmentation of vessel-like patterns using mathematical morphology and curvature evaluation, *IEEE Trans. Image Processing*, **10**, 1010–1019 (2001).

30. C. Wiedemann, External evaluation of road networks, *ISPRS Arch.*, **34**, 93–98 (2003).

31. J. Canny, A computational approach to edge detection, *IEEE Trans. PAMI*, **8**, 679–698 (1986).

32. N. Otsu, A threshold selection method from gray-scale histogram," *IEEE Trans. Syst., Man Cybernetics*, **9**, 62–66 (1979).